Structural correlations and phase separation in binary mixtures of charged and neutral colloids

Elshad Allahyarov[1, a)] and Hartmut Löwen[2]

[1)] *Theoretical Department, Joint Institute for High Temperatures,*

Russian Academy of Sciences (IVTAN), 13/19 Izhorskaya street, Moscow 125412,

Russia

[2)] *Institut für Theoretische Physik II: Weiche Materie, Heinrich-Heine Universität Düsseldorf,*

Universitätstrasse 1, 40225 Düsseldorf, Germany

(*Electronic mail: elshad.allahyarov@case.edu)

(Dated: 16 September 2022)

Structural correlations between colloids in a binary mixture of charged and neutral spheres are calculated using computer simulations of the primitive model with explicit microions. For aqueous suspensions in a solvent of large dielectric constant, the traditional Derjaguin-Landau-Vervey-Overbeek (DLVO) theory of linear screening, supplemented with hard core interactions, reproduces the structural correlations obtained in the full primitive model quantitatively. However for lower dielectric contrast, the increasing Coulomb coupling between the counterions and charged colloids results in strong deviations. We find a fluid-fluid phase separation into two regions either rich in charged or rich in neutral colloids which is not reproduced by DLVO theory. Our results are verifiable in scattering or real-space experiments on charged-neutral mixtures of colloids or nanoparticles.

[a)]Also at Institut für Theoretische Physik II: Weiche Materie, Heinrich-Heine Universität Düsseldorf, Universität-strasse 1, 40225 Düsseldorf, Germany; Also at Department of Physics, Case Western Reserve University, Cleveland, Ohio 44106-7202, United States

I. INTRODUCTION

There are, in principle, two mechanisms to stabilize colloidal suspensions against irreversible flocculation, namely charge-stabilization and steric stabilization[1–3]. In the former case, the colloidal particles are highly charged releasing counterions into the solvent such that they repel each other by electrostatics which is traditionally described by a screened Coulomb interaction. In the latter situation of steric stabilization, the colloidal particles are typically coated with polymer brushes causing repulsive entropic interaction forces which stabilize against flocculation. While the effective interactions and structural correlations in strongly interacting colloidal fluids are by now well-understood in one-component or even polydisperse systems of either charged[4–10] or neutral colloidal spheres[11–13], much less is known about binary mixtures of charged and neutral particles. Such binary neutral-charged systems occur frequently in mixtures of colloids with nanoparticles culminating in the charged nanoparticle-halo effect around neutral colloids which provides colloidal stabilization[14–28]. Moreover, in ordinary mixtures of charged colloids the particle charge can be tuned by the pH of the solution[29–31] such that one component stays charged and the other can become neutral close to the isoelectric point realizing a charged-neutral colloidal system. Further examples are neutral spherical vesicles exposed to charged colloids[32] and mixtures of charged nanoparticles and neutral spherical bacteria[33].

About 30 years ago, first theoretical calculations were performed for a binary mixture of charged and neutral spheres[34]. The results were based on a Yukawa model for the interaction between charged particles and a simple excluded volume hard sphere interaction between the charged-neutral and neutral-neutral spheres as predicted by standard DLVO-theory of linear screening applied to such a mixture. Liquid integral equation closures were then used to compute the partial pair correlation functions[23,31,34–36]. These studies with effective pairwise interactions give some first insight into the structural correlations but neglect nonlinear effects[37–39] beyond linear screening. In general the latter cause effective many-body interactions between the colloids[40,41]. While earlier studies have employed approximate Poisson-Boltzmann theory (see, e.g. Ref.[38]) and local classical density functional theory for the inhomogeneous counterions in

the field created by the charged colloids[37,39,42–44], it has become possible by now to calculate effective interactions and pair correlations with explicit counterions based on the primitive model (PM) approach of electrolytes[45–53] which includes full nonlinear screening and Coulomb correlations. Though there are simulations for charged mixtures[54–57] and even for oppositely charged colloids[55,58], to the best of our knowledge a mixture of charged and neutral colloids has not yet been simulated using the primitive model approach with explicit microions on a large scale. The binary colloidal mixture considered in this work can be assumed as a particular case of the charge regulated colloidal system investigated in Ref.[59] using mean-field formulation.

In this paper we close this gap and present computer simulations data for charged and neutral colloidal mixtures and extract their partial pair correlation functions. Complementary to earlier studies of the colloidal halo effect[15–20,22], we focus on the case of comparable hard core radii of the two colloidal spheres. Here, we find that the traditional Yukawa-hard sphere model is sufficient to describe the pair correlations in aqueous suspensions where the dielectric constant (or relative permittivity) ε of the solvent is pretty high (about 80 for water at room temperature). However, in less polar solvents when ε is reduced by an order of magnitude, the Coulomb coupling without screening between the charge species is getting much stronger resulting in nonlinear screening effects. In this study we show that for $\varepsilon = 8$, the standard Yukawa-hardcore interaction model as proposed in[34] cannot be applied any longer to a charged-neutral mixture. There are significant deviations in the pair correlations. Moreover we predict the existence of fluid-fluid phase separation as documented by divergence in the partial static structure factors at small wave vector. There are two regions either rich with charged or with neutral colloidal particles. This phase separation is absent within the traditional DLVO-model when combined with excluded volume interactions.

The paper is organized as follows. In section II we describe the details of our primitive model simulations for the binary colloidal system. The description of the parameters used in the different runs is presented in section III. The results obtained for the partial pair correlation functions, as well as the structure factors, are discussed in section IV with supplementary snapshots from the simulation boxes documenting phase separation for high Coulomb couplings without screening. In section V we explore the role of the core size of neutral colloids on the correlations and we conclude in section VI.

II.   DETAILS OF THE PRIMITIVE MODEL

We consider a three-component binary colloidal suspension consisting of N_Z colloids of charge $q^{(Z)} = Ze$ and size σ_Z at positions $\vec{r}_i^{(Z)}$ ($i=1,...,N_Z$), N_z neutral colloids of zero charge $q^{(z)} = 0$ and size σ_z at positions $\vec{r}_j^{(z)}$ ($i=1,...,N_z$), and $N_c = ZN_Z$ monovalent counterions of charge $q^{(c)} = -e$ and size $\sigma_c = \sigma_Z/600$ at positions $\vec{r}_\ell^{(c)}$ ($\ell=1,...,N_c$). Here e is the absolute value of the electron charge. We fix the size ratio $\sigma_Z/\sigma_z=1$ to unity such that $\sigma_Z = \sigma_z = \sigma$, and the number ratio $N_Z/N_z=1$ to reduce parameter space. As a reference state we also consider a case $q^{(z)} = q^{(Z)}$ which corresponds to a two component system containing only one species of charged colloids and compensating counterions.

The pair interaction potentials between the species α and β with $\alpha, \beta \in \{Z, z, c\}$ are given as a combination of excluded volume and Coulomb interactions (in SI units),

$$V^{(\alpha\beta)}(r_{ij}) = \begin{cases} \infty\,, & \text{for } r_{ij} \leq \sigma_{\alpha\beta}\,, \\ q^{(\alpha)}q^{(\beta)}/\left(4\pi\varepsilon_0\varepsilon r_{ij}\right)\,, & \text{for } r_{ij} > \sigma_{\alpha\beta}\,, \end{cases} \tag{1}$$

where $\vec{r}_{ij} = \vec{r}_j^{(\alpha)} - \vec{r}_i^{(\beta)}$ with $i \in 1,...,N_\alpha$ ($\alpha = Z, z, c$) and $j \in 1,...,N_\beta$ ($\beta = Z, z, c$) is the distance between the two particles, $\sigma_{\alpha\beta} = (\sigma_\alpha + \sigma_\beta)/2$ is their additive hard core diameter, ε_0 is the vacuum permittivity, and ε is the relative permittivity of the suspension. For simplicity, we assume that ε is the same throughout the system in order to avoid image charge and dielectric boundary effects.

The following parameters characterize the intensity of interparticle interactions and counterion screening effects in binary colloidal systems:

- the total packing fraction η of the colloids, $\eta = \eta_Z + \eta_z$, where $\eta_Z = \pi N_Z \sigma^3/(6L^3)$, $\eta_z = \pi N_z \sigma^3/(6L^3)$, and L is the edge size of the cubic simulation box.

- the Debye-Hückel inverse screening length $\kappa = \sqrt{n_c e^2/(\varepsilon_0\varepsilon k_B T)}$ of counterions, where k_B is the Boltzmann constant, T is the temperature in the system, and $n_c = N_c/L^3$ is the microion number density. High/low κ values correspond to strong/weak counterion screening conditions.

- the Bjerrum length, $\lambda_B = e^2/(4\pi\varepsilon_0\varepsilon k_B T)$,

- the average particle-particle separation distance in the charged and neutral colloidal subsystems, $\bar{a}_{ZZ} = L\left(6/(\pi N_Z)\right)^{1/3}$ and $\bar{a}_{zz} = L\left(6/(\pi N_z)\right)^{1/3}$. In the current study, $\bar{a}_{zz} = \bar{a}_{ZZ}$ because we assume throughout this paper $N_z = N_Z$.

- the Coulomb coupling parameter in the charged subsystem with a screening length κ, $\Gamma_{ZZ}=Z^2 \exp(-\kappa \bar{a}_{ZZ})\lambda_B/a$, and without screening, $\Gamma_{ZZ}^*=Z^2\lambda_B/a$.

III.   PRIMITIVE MODEL SIMULATION PARAMETERS

We have simulated globally electroneutral binary colloidal mixture in a cubic box of an edge length L with periodic boundary conditions in all three Cartesian directions. Molecular Dynamics (MD) runs with a Langevin thermostat with a Langevin damping coefficient (also known as Langevin friction coefficient) $\xi=2\text{ps}^{-1}$ and a random force chosen from the Gaussian distribution of zero mean and mean-square components $2\xi k_B T/\Delta t_{MD}$ were performed in a constant NVT ensemble. The total particle numbers $N = N_Z + N_z + Nc$ and the simulation box lengths L are listed in Tables 1, 2, and 3, $V = L^3$, and T=300K[56,57,60,61]. In order to handle the long-ranged Coulomb interactions, we use the Lekner summation method[62–64] which takes the real-space particle coordinates as its only input. The equations of motion were integrated using the velocity Verlet algorithm with a time step of Δt_{MD}=0.25fs. In the first stage of simulations the system was equilibrated during initial 1 ns simulations which correspond to about from 4×10^6 MD time steps. The equilibration was verified by examining the distribution function of velocities and pair distribution functions of counterions and colloids, and by the convergence of the total potential energy of the system during each run. Once the system was fully equilibrated, the statistically averaged quantities necessary to characterize the behavior of colloids were gathered during the second stage of simulations (production runs) which lasted up to 10-20 ns corresponding to, on average, 10^8 MD steps. All equilibration and production runs were carried out using OpenMP parallel programming code on clusters with 24 nodes, and it usually took from 2 to 3 weeks to get final results for each run.

We produced 4 different primitive model simulation run series A_m, B_m, C_m, and D_m, m=1,2,3. Each run series consists of three runs: a reference state run with m=1 where all colloids are charged, a binary run with m=2 where one half of colloids are charged and the other half is neutral, and another reference run with m=3 which is similar to the run with m=2 but without neutral colloids. To distinguish the two reference states, the reference state with m=1 will be referred as a "fully charged state".

The run series differ in the values of η and κ. In total, the run series A_m had low η and low κ, the run series B_m had high η and low κ, the run series C_m had low η and high κ, and the run

TABLE I. Primitive model simulation parameters for the run series A_m, B_m, C_m, and D_m, m=1,2,3. The quantities listed in the first row are explained in the text. The binary composition is 1:1, thus each component has a packing fraction $\eta_Z = \eta_z = \eta/2$.

Runs	Z	z	N_Z	N_z	η	N_c	$\bar{a}_{ZZ}$	$\kappa\sigma$	Γ_{ZZ}	Γ_{ZZ}^*	ε	L/σ
A_1	100	100	500	500	0.1	100000	2.15	1.31	1.98	33	80	17.36
A_2	100	0	500	500	0.1	50000	2.71	0.92	2.17	26	80	17.36
A_3	100	-	500	0	0.05	50000	2.71	0.92	2.17	26	80	17.36
B_1	100	100	500	500	0.2	100000	1.70	1.85	1.81	42	80	13.76
B_2	100	0	500	500	0.2	50000	2.15	1.32	1.94	33	80	13.76
B_3	100	-	500	0	0.1	50000	2.15	1.32	1.94	33	80	13.76
C_1	100	100	500	500	0.1	100000	2.15	4.14	0.05	330	8	17.36
C_2	100	0	500	500	0.1	50000	2.71	2.93	0.09	262	8	17.36
C_3	100	-	500	0	0.05	50000	2.71	2.93	0.09	262	8	17.36
D_1	100	100	500	500	0.2	100000	1.70	5.87	0.02	418	8	13.76
D_2	100	0	500	500	0.2	50000	2.15	4.15	0.04	330	8	13.76
D_3	100	-	500	0	0.1	50000	2.15	4.15	0.04	330	8	13.76

series D_m had high η and high κ. Simulation parameters for all runs are collected in Table I. To achieve high values for κ in the run series C_m and D_m, i.e. low Debye screening lengths $r_D = 1/\kappa$, the relative permittivity ε of the solvent was decreased from 80 to 8. All simulations were carried out at room temperature T=293 K, and the colloidal diameter was fixed to σ=100 nm. For the run series A_m and B_m, the Bjerrum length was λ_B=0.0071σ, whereas for the run series C_m and D_m, λ_B=0.071σ.

For each PM run listed in Table I, we also carried out corresponding binary Yukawa-DLVO system simulations[34] with no explicit counterions. The pair interaction potentials are given within DLVO-like theory as,

$$V^{(\alpha\beta)}(r_{ij}) = \begin{cases} \infty\,, & \text{for } r_{ij} \leq \sigma\,, \\ \dfrac{q^{(\alpha)}\exp(\kappa\sigma/2)}{1+\kappa\sigma/2}\dfrac{q^{(\beta)}\exp(\kappa\sigma/2)}{1+\kappa\sigma/2}\dfrac{\exp(-\kappa r_{ij})}{4\pi\varepsilon_0\varepsilon r_{ij}}\,, & \text{for } r_{ij} > \sigma\,, \end{cases} \tag{2}$$

where the values for the bare colloidal charges $q^{(\alpha)}$ and $q^{(\beta)}$, $\alpha,\beta = Z,z$, and for the inverse screening length κ are given in Table II.

TABLE II. Yukawa-DLVO model simulation parameters corresponding to the PM run series A_m, B_m, C_m, and D_m, m=1,2,3. The runs are labeled with an additional "Y".

Runs	Z	z	N_Z	N_z	η	$\kappa\sigma$	ε	L/σ
A_1Y	100	100	500	500	0.1	1.31	80	17.36
A_2Y	100	0	500	500	0.1	0.92	80	17.36
A_3Y	100	-	500	0	0.05	0.92	80	17.36
B_1Y	100	100	500	500	0.2	1.85	80	13.76
B_2Y	100	0	500	500	0.2	1.32	80	13.76
B_3Y	100	-	500	0	0.1	1.32	80	13.76
C_1Y	100	100	500	500	0.1	4.14	8	17.36
C_2Y	100	0	500	500	0.1	2.93	8	17.36
C_3Y	100	-	500	0	0.05	2.93	8	17.36
D_1Y	100	100	500	500	0.2	5.87	8	13.76
D_2Y	100	0	500	500	0.2	4.15	8	13.76
D_3Y	100	-	500	0	0.1	4.15	8	13.76

IV. PM SIMULATION RESULTS

A. Run series A_m and B_m for weak counterion screening

The PM and Yukawa-DLVO simulation snapshots for the run series A_m and B_m with low $\kappa\sigma \leq$ 1.85, i.e. weak counterion screening, are shown in Figure 1. The PM snapshot for the run B_1 is separately shown in Figure 2 to make the counterions visible, which otherwise are hardly visible in Figure 1. A visual inspection of the PM and the corresponding Yukawa-DLVO runs reveals that in both cases the charged and neutral colloids are randomly distributed across the system boundaries. This is an indirect indication of the mutual repulsion between the charged colloids.

A detailed picture of the distribution of colloids around a target colloid can be achieved by calculating the partial pair correlation functions $g_{ij}(r)$, i,j=Z,z, for the charged colloids and neutral colloids. These functions for the run series A_m, B_m, A_mY, and B_mY are shown in Figure 3. Interestingly, both PM and the corresponding Yukawa-DLVO runs show similar trends for the charged colloid $g_{ZZ}(r)$, such as the position of the first maximum r_{max} in $g_{ZZ}(r)$ for the fully charged state
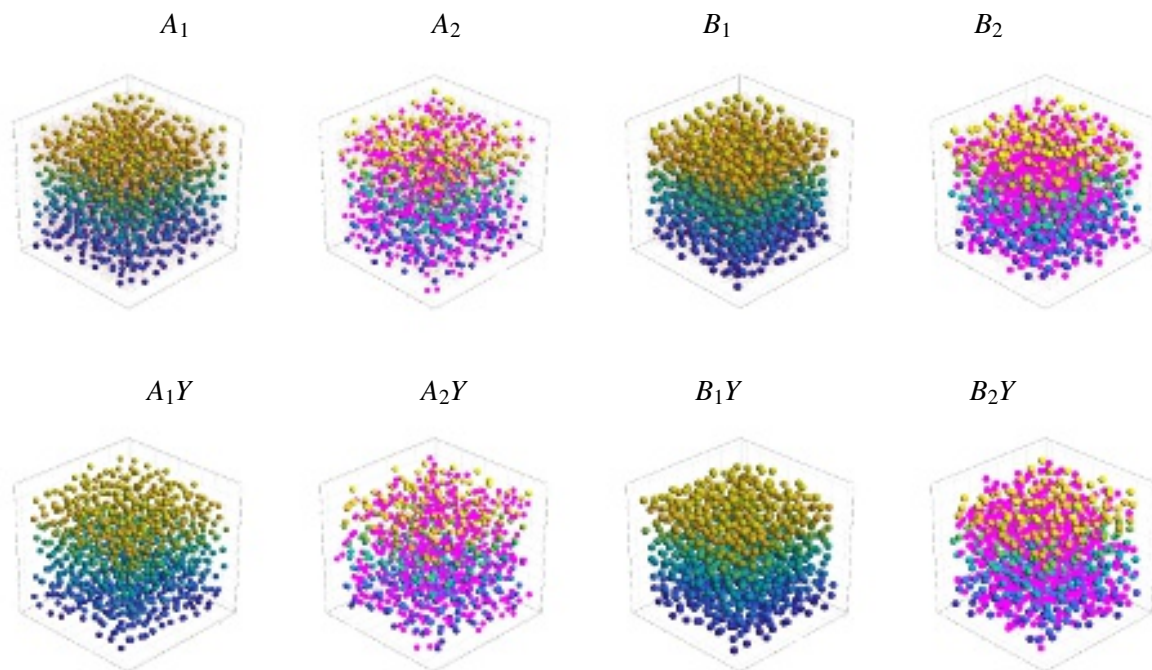
FIG. 1. Simulation snapshots from the PM runs A_1, A_2, B_1, B_2 (upper row), and their counterpart Yukawa-DLVO runs A_1Y, A_2Y, B_1Y, B_2Y (bottom row). A color gradient from blue to orange is used for the charged colloids according to their altitude in the cell. Neutral colloids are shown as pink spheres. The PM counterions are shown as scattered red dots.

system (see the green line) shifts to the right for the binary system run (see the black line). The reference runs (see the pink line) have their r_{max} in $g_{ZZ}(r)$ nearly at the same distance r for the binary runs. Such shifting of r_{max} to the right from the fully charged state run to the binary and reference runs clearly signals about a stronger repulsion between the charged colloids in the latter compared to the former run. The stronger repulsion originates from the decreasing of the inverse screening length κ, i.e. from the weaker screening of the colloids in the binary and reference runs.

The PM and Yukawa-DLVO simulated $g_{Zz}(r)$ and $g_{zz}(r)$ for the charged-neutral and neutral-neutral colloids, see the blue line and red lines Figure 3, correspondingly, look practically the same, except having major differences at smaller separations r. At $r < 1.1\sigma$, the PM simulated $g_{zz}(r)$ and $g_{Zz}(r)$ show an upturn and reach higher contact values at $r = \sigma$, whereas the related contact values in the Yukawa-DLVO results are around one. The higher contact value in the PM simulated $g_{zz}(r)$ is an indication of a pairwise clustering between neutral colloids. We assume that it is the entropic force $F_{ent}(r)$ of the counterions acting on the neighboring neutrals, which pushes

8
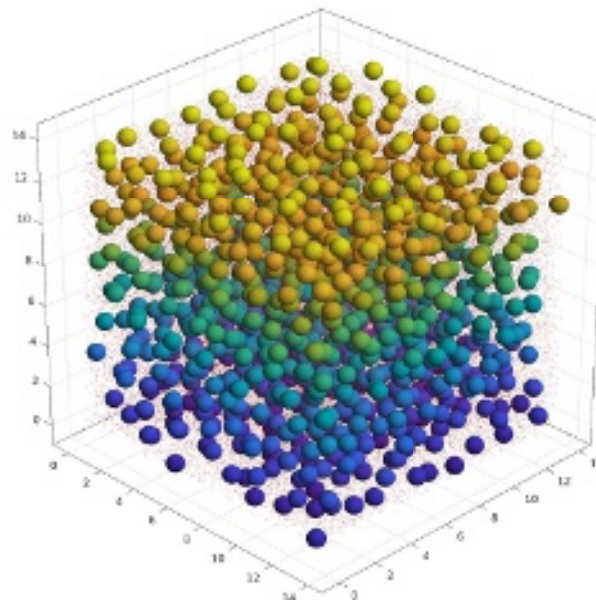
FIG. 2. Simulation snapshot from the PM run B_2.

them together. The definition of the counterion entropic force acting on the colloids is introduced in Appendix A. This force, as shown in Figure 9, depends both on the neutral colloid size σ_z, and on the coupling parameter between the charged colloid and its counterions, or, equivalently, on $\kappa\sigma_Z$. A larger neutral colloid in the vicinity of a strongly screened colloid endures a stronger and repulsive entropic force. As a result, if a pair of neutral colloids i and j are surrounded by the charged colloids, the entropic forces $F_{ent}^{(i)}$ and $F_{ent}^{(j)}$ acting on them will induce a mutual attraction. The latter, however, should not be confused with the classical depletion force in binary systems of neutral colloids. As shown by Mao et. al.[69], the depletion attraction in such binary neutral systems has a range of 0.2-0.3σ_b for the size ratio σ_b/σ_s=10 (σ_b is the size of the bigger colloid, and σ_s is the size of the smaller colloid) and the packing fraction of the smaller component η_s=0.1. For the simulation runs shown in Tables 1 and 3, however, the counterions are much smaller and have negligible packing fraction, σ_Z/σ_c=600, and $\eta_c \approx 10^{-6}$. The entropic forces calculated analytically and shown in Appendix A, and simulated for a pair of neutrals in the binary system and shown in Appendix D, have a range of 2σ_Z. In other words, the attraction between the neutral colloids, whereas it seems like a depletion attraction, in fact is a 'counterion depletion' force which

9
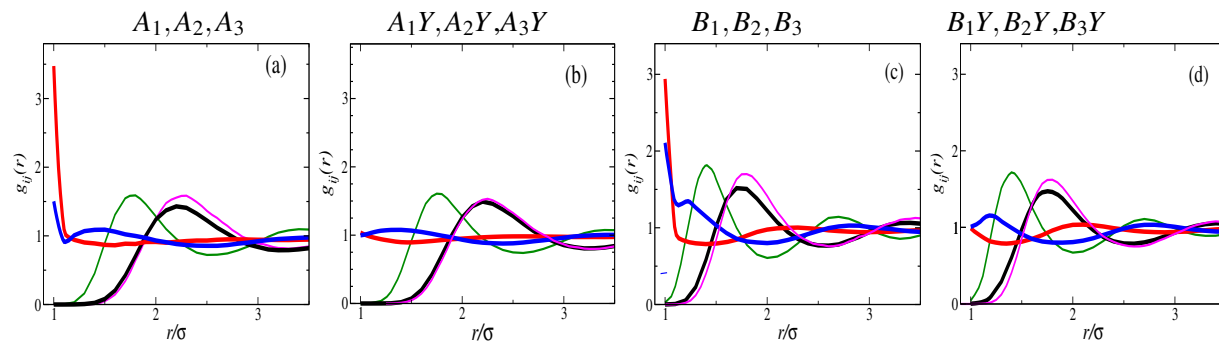
FIG. 3. (Color in online) Partial pair correlations $g_{ij}(r)$ for the PM run series A_m and B_m from Table 1, and for the Yukawa-DLVO run series A_mY and B_mY from Table 2. (a)- the run series A_m, (b)- the run series A_mY, (c)- the run series B_m, and (d)- the run series B_mY. The case m=1 corresponds to a fully charged state where all colloids have a charge Z=100, and the correlation functions $g_{ZZ}(r)$ are shown as green lines. The case m=2 corresponds to a binary mixture of the charged and neutral colloids with Z=100 and z=0, respectively. For this case, the corresponding correlation functions $g_{ZZ}(r)$ for the charged colloid-charged colloid are shown as black lines, $g_{Zz}(r)$ for the charged colloid-neutral colloid are shown as blue lines, and $g_{zz}(r)$ for the neutral colloid-neutral colloid are shown as red lines. The case m=3 corresponds to the reference runs with no neutral colloids, and the corresponding correlation functions $g_{ZZ}(r)$ are shown as pink lines.

stems from the counterion orbitals of the neighboring charged colloids. Note that this entropic force is absent in the Yukawa-DLVO model.

The average number of neutral colloids in the cluster they form can be evaluated from the integration of the calculated $g_{zz}(r)$,

$$\bar{N}_{cz} = 4\pi \frac{N_z}{V} \int_{\sigma}^{r'} g_{zz}(r)r^2 dr \tag{3}$$

where r' is the position of the first minimum of $g_{zz}(r)$. For the red lines in Figure 3(a) and (c), we get $\bar{N}_{cz}$=2 and $\bar{N}_{cz}$=3, respectively. These numbers confirm that neutral colloids indeed experience a pairwise clustering effect. An interesting question is whether such pairwise clustering is robust against the packing fraction η. To answer this question we carried low-η simulations with η=0.01. The obtained results for $g_{ij}(r)$ are reported in Figure 11(a) in Appendix C. Eq.(3) applied to the red line in Figure 11(a) reveals $\bar{N}_{cz} \approx 1$, i.e. no clustering in the neutral component at all.

There is an upturn in $g_{Zz}(r)$ at small separations in the PM binary simulations, which does not appear in the Yukawa-DLVO binary simulations. To understand the origin of such short-range association between charged and neutral colloids, we analyze the radial distribution of counterions,

$\rho_c^{(i)}(r)$, around the colloids in Appendix B. As can be seen from Figure 10, both the charged and neutral colloids are wrapped by the screening counterions. This gives rise to effective attraction between charged and neutral particles via counterion depletion in the binary PM runs A_2 and B_2 in Figure 3.

In total, because the upturn in $g_{zz}(r)$ and $g_{Zz}(r)$ appears at very small separations, such pairing (or association) is not easy to detect visually in the simulation snapshots in Figure 1.
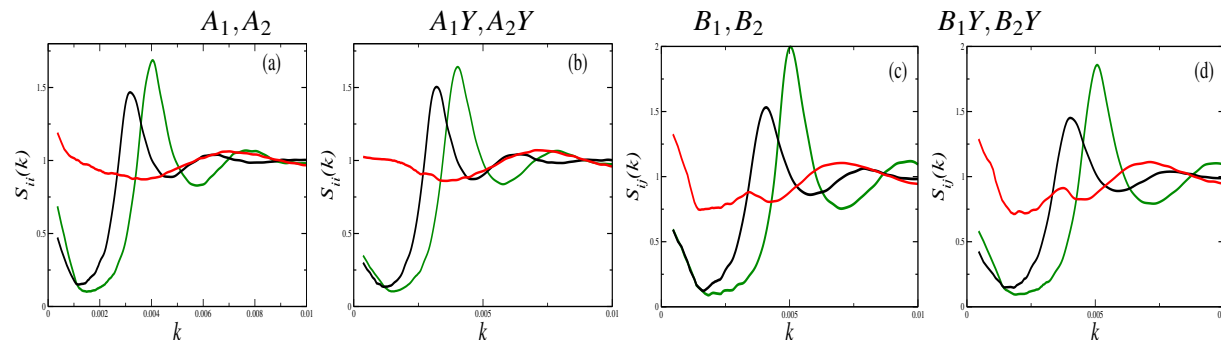

FIG. 4. (Color in online) Structure factors $S_{ij}(k)$ for the PM runs A_1 and A_2 (a), B_1 and B_2 (c), and Yukawa-DLVO runs A_1Y and A_2Y (b), B_1Y and B_2Y (d). Green lines- $g_{ZZ}(r)$ for the fully charged state runs A_1, B_1, A_1Y, B_1Y. Black lines- $g_{ZZ}(r)$, and red lines- $g_{zz}(r)$ for the binary runs A_2, A_2Y, B_2, B_2Y.

In Figure 4 we analyze the partial colloid-colloid structure factors $S_{ij}(k)$. The colors used for the lines are the same as in Figure 3. There are only from light to negligible differences between the PM and Yukawa-DLVO data, which indicates that the structural correlations between the charged colloids and between the neutral colloids, are nearly the same in both simulation protocols. The calculated $S_{ij}(k)$ have non-diverging values at small-k, which is pertinent to the random (i.e. no long-range clustering) distribution of colloids in the system and indicates a finite compressibility.

B. Run series C_m and D_m for strong counterion screening

The PM and Yukawa-DLVO simulation snapshots for the run series C_m and D_m with high inverse screening $\kappa\sigma \geq 2.93$, i.e. strong counterion screening, are shown in Figure 5. The PM and Yukawa-DLVO snapshots look similar for the fully charged state runs C_1 and C_1Y, and for D_1 and D_1Y, however they strongly differ for the binary runs C_2 and C_2Y, and for D_2 and D_2Y. The PM snapshots exhibit demixing and clustering in the binary system, whereas such clustering is absent in the binary Yukawa-DLVO runs.
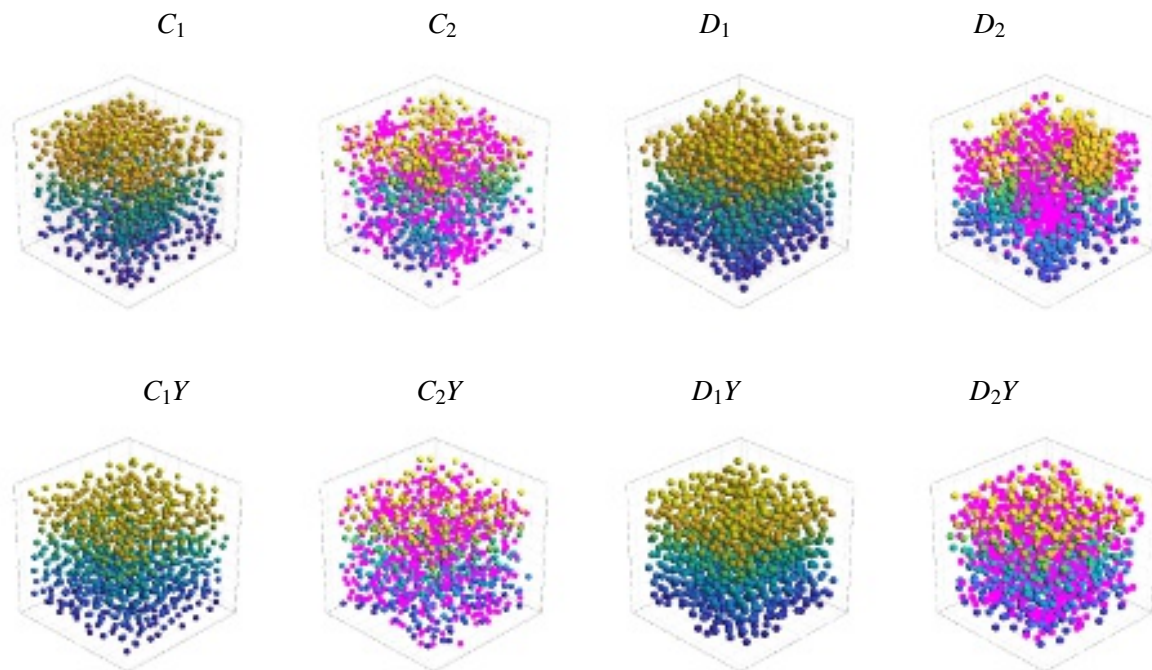
FIG. 5. Simulation snapshots from the PM runs C_1, C_2, D_1, D_2 (upper row), and the corresponding Yukawa-DLVO runs C_1Y, C_2Y, D_1Y, D_2Y (bottom row). Neutral colloids are shown as pink spheres. The PM counterions are shown as scattered red dots.

Partial pair correlation functions $g_{ij}(r)$, presented in Figure 6, also confirm the clustering in the binary PM runs. First, the height of the first maximum in the PM fully charged state $g_{ZZ}(r)$ is smaller than its value in the corresponding Yukawa-DLVO fully charged state, compare the green lines in Figure 6(a) and (b), and in (c) and (d). We believe that this happens because of much stronger colloidal charge screening in the PM runs. As a result, strongly screened colloids can easily approach each-other up to small separations in the PM fully charged state runs. The same scenario is valid for the $g_{ZZ}(r)$ in the binary PM runs, compare the black lines in Figure 6(a) and (b), and in (c) and (d). The position of the first maximum r_{max} in $g_{ZZ}(r)$ in the PM binary run is shifted to the left compared to the corresponding Yukawa-DLVO binary run. Moreover, the PM simulated black lines are above the line $g = 1$ for the entire range of the separation distance r for the run D_2, and for $r > r_{max}$ for the run C_2, which is a direct indication of the clustering of binary PM runs.

Second, as seen from the blue lines for $g_{Zz}(r)$ in Figure 6(a) and (c), there is a repulsion between the charged and neutral colloids resulting in $g_{Zz}(r) < 1$ for $r \leq 4\sigma$. This can be viewed as another

confirmation of the demixing in the PM binary runs. In opposite to it, the Yukawa-DLVO binary runs exhibit the charged colloid-neutral colloid association at low separation distances where $g_{Zz}(r) > 1$, see Figure 6(b) and (d). A similar association was observed for the run series A_m and B_m in previous section.

Third, the binary PM results for the neutral-neutral pair correlation function $g_{zz}(r)$, see the red curves in Figure 6(a) and (c), completely differ from the corresponding Yukawa-DLVO results in Figure 6(b) and (d). Whereas the latter shows no clustering at all, the former indicates a strong coagulation effect in the system of neutral colloids with high contact values $g_{zz}(\sigma) \approx 6$. Compared to the $g_{zz}(r)$ lines in Figure 3 for the runs A_2 and B_2 with $\varepsilon=80$, simulation data in Figure 6 show a stronger neutral-neutral clustering for the runs C_2 and D_2 with $\varepsilon=8$. This is in line with the prediction of the analytical expression for the entropic force in the framework of Yukawa orbitals for the counterion profiles given in Appendix A. As shown in Figure 9(a), the force $F_{ent}(r)$ is much stronger for the run D_2 with a higher coupling parameter $\Gamma^*_{ZZ}=330$, compared to the force $F_{ent}(r)$ for the run B_2 with $\Gamma^*_{ZZ}=3$.

We again apply Eq.(3) to the calculated $g_{zz}(r)$ to get the average number of neutral colloids in the cluster. For the red lines in Figure 6(a) and (c) we get $\bar{N}_{cz}=25$ for the run C_2 and $\bar{N}_{cz}=80$ for the run D_2. This is an indication of a strong coagulation in the neutral component of the system. Compared to the values of $\bar{N}_{cz}$ for the runs A_2 and B_2 in the previous section, we see that stronger electrostatic coupling in the charged subsystem of colloids provides stronger clustering in the neutral subsystem of the binary mixture.

A similar cluster size procedure using Eq.(3) can be also applied to the charged colloid pair correlation function $g_{ZZ}(r)$, i.e. to the black lines in Figure 6(a) and (c). In this case we get $\bar{N}_{cz}=37$ for the run C_2 and $\bar{N}_{cz}=82$ for the run D_2. It should be noted that the clustering observed in the neutral component disappears in systems with low packing fraction η. Figure 11(b) in Appendix C contains the simulated pair correlation functions $g_{ij}(r)$ for a system similar to the run C_2 but with η reduced 10 times, $\eta=0.01$. The red line corresponding to $g_{zz}(r)$ fluctuates around the line $g=1$, and Eq(3) applied to this line reveals $\bar{N}_{cz} \approx 1$, i.e., no clustering in the neutral component.

To analyze the origin of the observed clustering in binary PM runs C_2 and D_2, additional two-colloid simulations were carried out for the runs D_1 and D_2, see Appendix D for details. The calculated pair interaction potentials show a repulsive interaction $U_{ZZ}(r)$ between the charged colloids for the PM runs D_1 and D_2, see the the upper row in Figure 12(a), and even much stronger repulsion $U^Y_{ZZ}(r)$ in the Yukawa-DLVO runs D_1Y and D_2Y, see the bottom row in Figure 12(a).

As seen from the upper row in Figure 12(b), the calculated cross interaction potential $U_{Zz}(r)$ between the charged colloid and a neutral colloid is always positive. It has a shallow minimum at small separations and a repulsive barrier at larger distances. This repulsive barrier is the main reason why neutral colloids avoid the neighborhood of the charged colloids in the PM binary runs C_2 and D_2, as seen from the blue lines for $g_{Zz}(r)$ in Figure 6(a) and (c). Opposite to it, the Yukawa-DLVO cross term interaction potential $U_{Zz}^Y(r)$ is always attractive, as seen from Figure 12(b), bottom row. This explains the charged colloid-neutral colloid association for the binary Yukawa-DLVO runs in Figure 6(b) and (d).

The neutral-neutral interaction potential $U_{Zz}(r)$ is attractive (by about 3 k_BT) in the PM run D_2, whereas $U_{Zz}^Y(r)$ is very weak in the Yukawa-DLVO run D_2Y, see Figure 12(c) upper and bottom rows. This result explains the observed clustering of the neutrals in the snapshots in Figure 5 for the binary PM runs C_2 and D_2.
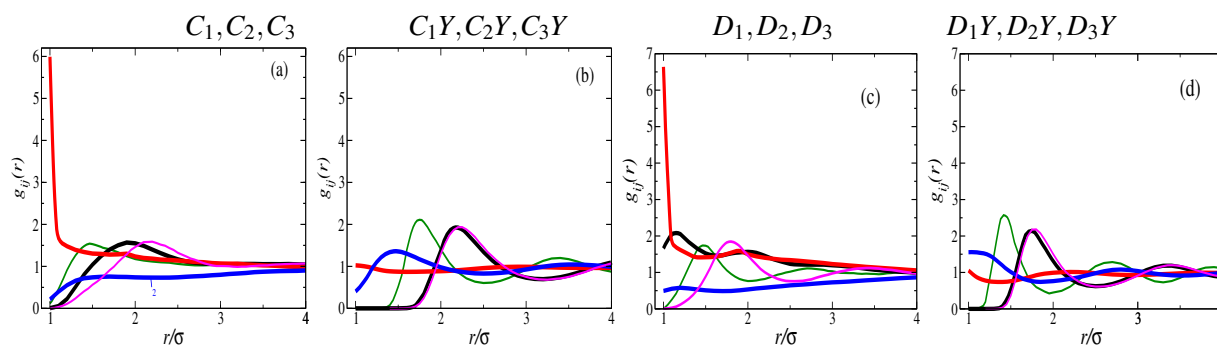

FIG. 6. (Color in online) Partial pair correlations $g_{ij}(r)$ for the PM run series C_m and D_m from Table 1, and for the Yukawa-DLVO run series C_mY and D_mY from Table 2. (a)- the run series C_m, (b)- the run series C_mY, (c)- the run series D_m, and (d)- the run series D_mY. The case $m=1$ corresponds to a fully charged state where all colloids have a charge $Z=100$, and the correlation functions $g_{ZZ}(r)$ are shown as green lines. The case $m=2$ corresponds to a binary mixture of the charged and neutral colloids with $Z=100$ and $z=0$, respectively. For this case, the corresponding correlation functions $g_{ZZ}(r)$ for the charged colloid-charged colloid are shown as black lines, $g_{Zz}(r)$ for the charged colloid-neutral colloid are shown as blue lines, and $g_{zz}(r)$ for the neutral colloid-neutral colloid are shown as red lines. The case $m=3$ corresponds to the reference runs with no neutral colloids, and the corresponding correlation functions $g_{ZZ}(r)$ are shown as pink lines.

The PM and Yukawa-DLVO simulated structure factors $S_{ij}(k)$ are plotted in Figure 7, The PM simulated $S_{zz}(k)$ for thew neutral component has strong up-turn in the low-k region for the binary
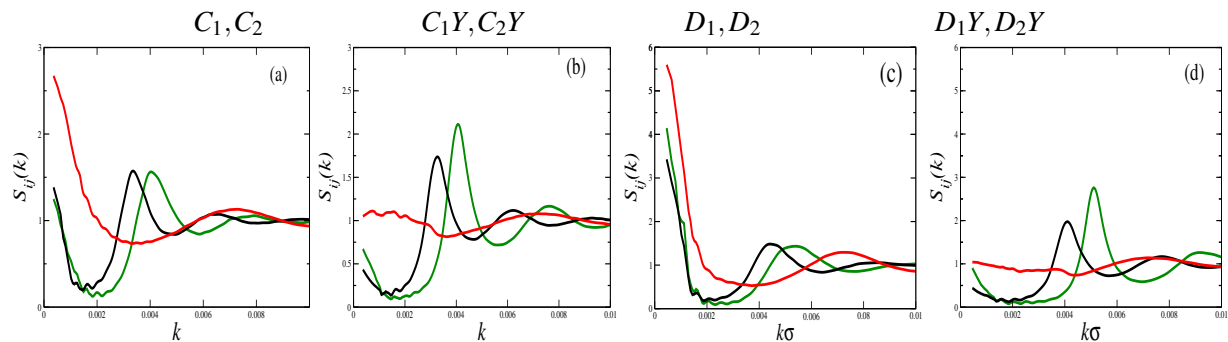
FIG. 7. (Color in online) Structure factors $S_{ij}(k)$ for the PM run series C_m and D_m ((a) and (c)), and for the Yukawa-DLVO run series C_mY and D_mY ((b) and (d)). Green lines- $g_{ZZ}(r)$ for the fully charged state runs C_1, C_1Y, D_1, D_1Y. Black lines- $g_{ZZ}(r)$, and red lines- $g_{zz}(r)$ for the binary charged-neutral runs C_2, C_2Y, D_2, D_2Y.

runs C_2 and D_2. Such divergence, though still finite in value, in practice is an indication of a *phase separation* in the neutral component. Since all partial structure factors are coupled, we expect that this indicates a global phase separation in a charged colloid-rich and charged colloid-poor fluid. At the same time, no such clustering (nor any sign of phase separation) is detected in the binary Yukawa-DLVO runs C_2Y and D_2Y in Figure 7.

Radial distribution functions $\rho_c^{(Z)}(r)$ and $\rho_c^{(z)}(r)$ of the counterions around the colloids for the runs series C_m and D_m are presented in Figure 10. Due to the strong Coulomb coupling of counterions to the charged colloids, there are less counterions near neutral colloids than in the bulk, which is another indication of the demixing in the charged-neutral binary system.

V. NEUTRAL COLLOID SIZE EFFECT ON THE CLUSTERING EFFECT

The entropic force of the screening counterions acting on neutral colloids, see Eq.(4) in Appendix A, explicitly depends on the core radius σ_z of the latter. Therefore, the bigger the neutral colloid, the stronger the entropic force they endure. When a pair or several neutral colloids are surrounded by the charged colloids, it is natural to expect that the entropic force of the counterions will force the neutrals to stick to each other. For smaller σ_z the entropic force will be weak, and, as a result, neutral colloids might evade the entropic pressure of the counterions and attain random distribution across the system. In order to verify this suggestion, the PM binary run A_2, for which a pairwise clustering in $g_{zz}(r)$ was detected at low separations, see the red line in Figure 3(a), is
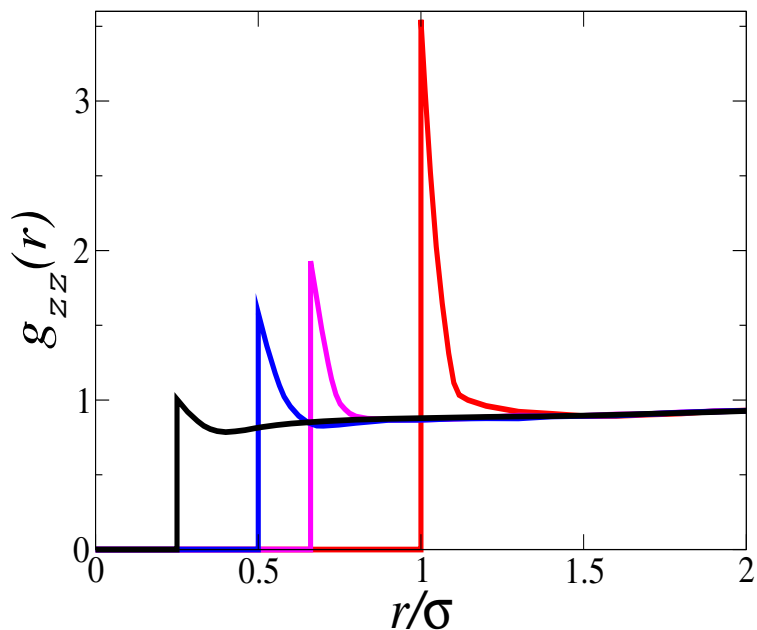
FIG. 8. (Color in online) PM simulated pair correlations functions $g_{zz}(r)$ for neutral colloids for the binary runs A_2 (red line), E_1 (pink line), E_2 (blue line), and E_3 (black line). The run parameters are given in Table III.

TABLE III. PM binary run parameters for A_2, E_1, E_2, and E_3.

Runs	Z	z	N_Z	N_z	η	N_c	$\bar{a}_{ZZ}$	$\kappa\sigma$	Γ_{ZZ}	σ/σ_n	ε	L/σ
A_2	100	0	500	500	0.1	50000	2.71	0.92	2.17	1.0	80	17.36
E_1	100	0	500	1700	0.1	50000	2.71	0.92	2.17	1.5	80	17.36
E_2	100	0	500	4000	0.1	50000	2.71	0.92	2.17	2.0	80	17.36
E_3	100	0	500	32200	0.1	50000	2.71	0.92	2.17	4.0	80	17.36

chosen as a reference system with $\sigma/\sigma_z=1$, and three additional runs E_1-E_3 with the size ratio $\sigma/\sigma_z=1.5$, 2, and 4, see Table III, were carried. While the size of neutral colloids is decreased, their number N_z was increased in order to keep their total packing fraction fixed to $\eta/2=0.05$, provided that the charged colloids keep their packing fraction fixed to $\eta/2=0.05$.

Simulated pair correlation functions $g_{zz}(r)$, presented in Figure 8, confirm that the smaller the neutral colloid, the weaker is the short-range clustering in the neutral component. When the neutral colloid is 4 times smaller than the charged colloid, the short-range clustering completely disappears, see the black line in Figure 8.

16

VI.   CONCLUSIONS

To summarize, we have calculated the pair correlations in a binary mixture of charged and neutral colloids using the primitive model with explicit counterions and compared the results to the Yukawa-DLVO model. We found that the traditional DLVO based approach is sufficient to describe the pair correlations in aqueous suspensions with high dielectric constant. However, in less polar solvents with reduced permittivity, the Coulomb coupling without screening between the charge species is getting much stronger which results in nonlinear screening effects. In this case the Yukawa-DLVO approach completely fails to describe the PM results for the pair correlations. We predict, for the first time, indications for a fluid-fluid phase separation in such strongly nonlinear systems. Our simulations show that there are two regions either rich with charged or with neutral colloidal particles.

Additional two colloid simulations were staged to calculate interaction potentials between colloids in the binary runs that show fluid-fluid phase separation. We found that the interaction between the charged colloids is strongly repulsive, whereas it is moderately repulsive between the charged and neutral colloids. More interestingly, the interaction between neutral colloids is strongly attractive. We believe that the latter is the main reason for the fluid-fluid phase separation in the simulated binary system with strong Coulomb coupling.

Finally we remark that the predicted phase separation can in principle be verified in experiments on binary mixtures of charged and neutral colloids. There are various techniques to prepare such mixtures in the colloidal size domains and the clustering can be measured using either real-space or low-angle scattering techniques. However, to find phase separation requires a fine tuning of the parameters (such as density and charge number) so that such an experiment might not be straightforward.

Appendix A: Electrostatic and Entropic Forces in Binary Mixtures

In the PM simulations, the excluded volume of the colloids initiates entropic forces arising from the contact density of counterions and neutral colloids on the target colloid surface. The entropic force acting on a i-th colloid of species α at the position $\vec{r}_i^{(\alpha)}$ with $i \in 1,...,N_\alpha$ ($\alpha = Z, z$) is defined as[60,61,65–68].

$$\vec{F}_{ent}^{(\alpha)}(\vec{r}_i^{(\alpha)}) = -k_B T \int_{S_i^{(\alpha)}} d\vec{f}\,\rho_\beta(\vec{r}) \tag{4}$$

where $\vec{f}$ is a surface normal vector pointing outwards the colloid's core, $S_i^{(\alpha)}$ is the surface of the hard core of the i-th colloid centered around $\vec{r}_i^{(\alpha)}$ with diameter $(\sigma_\alpha + \sigma_\beta)/2$, $\beta=z$ for neutral colloids, and $\beta=c$ for the counterions, and $\rho_\beta(\vec{r})$ is the density of particles of sort β around the i-th colloid.

In our previous paper[54] we derived a simple analytical expression for the entropic force acting on the colloid *1* of diameter σ_z from the counterion cloud of the colloid *2* of diameter σ_Z and charge Z assuming that the counterion density field around the charged particle *2* is approximated by a Yukawa orbital. The resulting entropic force is written as,

$$\frac{\vec{F}_{ent}(\vec{r})}{k_B T Z} = \left(\frac{\sigma_z}{2r_D} \cosh\left(\frac{\sigma_z}{2r_D} \right) - \sinh\left(\frac{\sigma_z}{2r_D} \right) \right) e^{-\frac{2r-\sigma_Z}{2r_D}} \frac{2r_D}{2r_D + \sigma_Z} \frac{r+r_D}{r^3} \vec{r} \tag{5}$$

where r_D is the Debye screening length in the system. As shown in Ref.[54] this simple theory describes the simulation results for a pair of colloids qualitatively well. There are two main and interesting facts to be noticed in Eq.(5). First, with the decrease of the Debye screening length r_D, which can be achieved by decreasing the dielectric permittivity ε in the system, the entropic force $F_{ent}(r)$ acting on the colloid *1* increases. Such increase is mostly related to the shape of the counterion profile described by the Yukawa orbital, which becomes steeper near the surface of the charged colloid at low permittivities ε. This is illustrated in Figure 9(a) for the runs B_2 and D_2 from Table 1. It is obvious that the entropic force acting on neutral colloids becomes stronger as the permittivity ε decreases from 80 to 8. Second, the entropic force $F_{ent}(r)$ acting on the neutral colloid correlates with the diameter σ_z of the latter. The smaller σ_z, the weaker $F_{ent}(r)$. This scenario is illustrated in Figure 9(b) for the runs A_2 from Table 1 and E_2 from Table 3.

The entropic force given by Eqs.(4) and (5), and shown in Figure 9, usually neglected in weakly charged colloidal systems, strongly modifies the colloidal interactions in highly charged and dense colloidal systems.
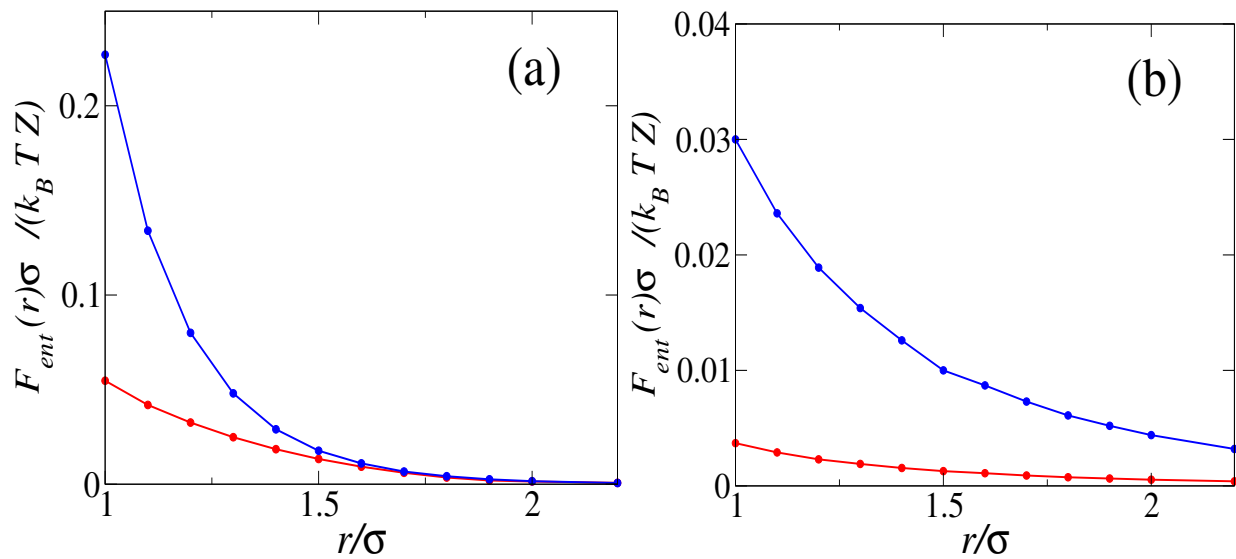
FIG. 9. (Color in online) Normalized entropic force $F_{ent}(r)$ from Eq.(5) acting on the neutral colloid from the counterion cloud of the neighboring colloid with charge Z and diameter σ_Z. Case (a): red line corresponds to $\kappa\sigma_Z=1.32$ taken from the run B_2 with $\varepsilon=80$, and blue line corresponds to $\kappa\sigma_Z=4.15$ taken from the run D_2 with $\varepsilon=8$. Case (b): blue line corresponds to $\kappa\sigma_Z=0.92$ taken from the run A_2 with neutral colloid diameter being the same as σ_Z, and red line corresponds to $\kappa\sigma_Z=0.92$ taken from the run E_2 with the neutral colloid diameter being twice smaller than σ_Z.

Likewise, the canonically averaged electrostatic force acting on the i-th colloid of species α is defined as,

$$\vec{F}_{elec}^{(\alpha)}(\vec{r}_i^{(\alpha)}) = \left\langle \sum_{\beta=Z,z,c} \sum_{j=1}^{N_\beta} \vec{F}^{(\alpha\beta)}(\vec{r}_i^{(\alpha)} - \vec{r}_i^{(\beta)}) \left(1 - \delta_{\alpha\beta}\,\delta_{ij}\right) \right\rangle_c \qquad (6)$$

where $\alpha = Z, z$ and $\beta = z, c$. The Kronecker delta functions in this expression nullify the self-interaction of colloids. Clearly, in Eq.(6) the electrostatic pair interaction forces $\vec{F}^{(\alpha\beta)}$ are defined as,

$$\vec{F}^{(\alpha\beta)}(\vec{r}_{ij}) = -\vec{\nabla}_{\vec{r}_{ij}} V^{(\alpha\beta)}(r_{ij}) = \frac{1}{4\pi\varepsilon_0} \frac{q^{(\alpha)} q^{(\beta)}}{\varepsilon r_{ij}^2} \frac{\vec{r}_{ij}}{r_{ij}} \qquad \text{for } r_{ij} > \sigma_{\alpha\beta} \qquad (7)$$

where $\vec{r}_{ij} = \vec{r}_i^{(\alpha)} - \vec{r}_i^{(\beta)}$.

Appendix B: Radial Distribution of Counterions Around Colloids

Radial distribution of counterions, $\rho_c^{(i)}(r)$, around the charged, $i=Z$, and neutral, $i=z$, colloids is defined as,

$$\rho_c^{(\alpha)}(r) = \left\langle \sum_{i=1}^{N_\alpha} \rho_c\left(\vec{r} - \vec{r}_i^{(\alpha)}\right) \right\rangle_\alpha \qquad (8)$$

where the averaged counterion density field,

$$\rho_c(\vec{r}) = \left\langle \sum_{\ell=1}^{N_c} \delta\left(\vec{r} - \vec{r}_\ell^{(c)}\right) \right\rangle_c \qquad (9)$$

parametrically depends on the fixed colloid positions $\rho_c(\vec{r}) \equiv \rho_c(\vec{r}, \{\vec{r}_i^{(Z)}, \vec{r}_j^{(z)}\})$, $\{\vec{r}_i^{(Z)}, \vec{r}_j^{(z)}, i = 1, ..., N_Z; j = 1, ...N_z\}$, where the counterion averaging $\langle \cdots \rangle_c$ and the colloid averaging $\langle \cdots \rangle_\alpha$ ($\alpha = Z, z$) are done for fixed colloid positions.

As seen from Figure 10, where the run series A_m and B_m are analyzed, the counterion density at the surface of neutral colloids in the PM binary runs is larger than in the bulk. This effect appears to be more solid for η=0.2 simulations. Because no counterions are originally associated with neutral colloids, it is the counterions stemming from the charged colloids that exist near neutral colloids. This conclusion is supported by the appearance of the minimum in the counterion distribution at around $r = 1.2\sigma$, see the red line, below which the charged colloid-neutral colloid association develops in the PM binary runs in Figure 3, see the blue line there.
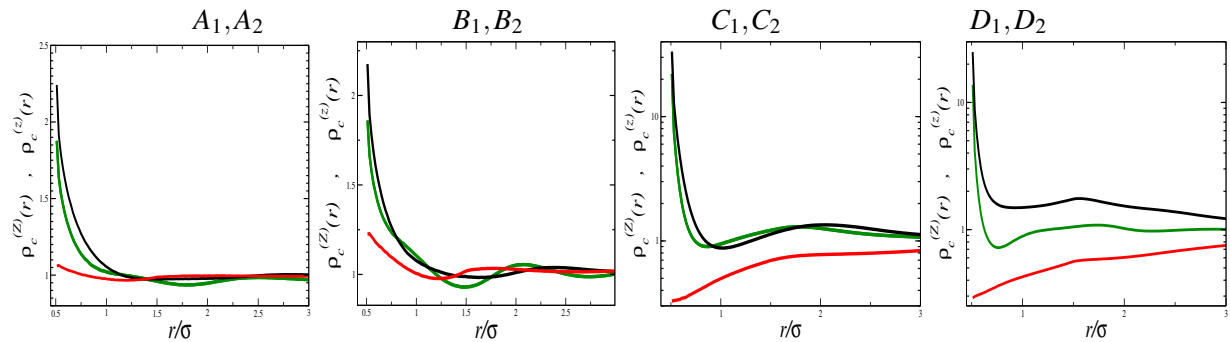

FIG. 10. (Color in online) Normalized radial distribution function $\rho_c^{(q)}(r)$ of counterions around the colloids for the run series X_m, m =1,2, X=A, B, C, D. Green lines- $q^{(Z)}$=100e for the fully charged state runs X_1, black lines- $q^{(Z)}$=100e, and red line- $q^{(z)}$=0 for the binary runs X_2.

For the run series C_m and D_m, there are less counterions near neutral colloids than in the bulk, see the monotonic increase of $\rho_c^{(z)}(r)$ from the distance $r = 0.5\sigma$ to $r = 3\sigma$. In other words, the

counterions are mostly localized to the regions of charged colloids. This is another indication of the demixing in the charged-neutral system. Another interesting factor is a much stronger screening of the colloidal charge in the binary PM run D_2 compared to the fully charged state run D_1, see the gap between these two lines in Figure 10. The reason for such stronger screening in D_2 is the stronger colloid clustering effect in the D_2 run. Larger clusters of charged colloids practically trap all their compensating counterions in and around them for effective screening. This suggestion is also supported by the differences in the black line (g_{ZZ} for the binary PM run D_2) and green line (g_{ZZ} for the fully charged state PM run D_1) in Figure 6.

Appendix C: Colloid-Colloid Pair Correlation Functions at Low $\eta = 0.01$

We calculated colloid-colloid pair correlation functions $g_{ij}(r)$ for a binary colloidal system with Z=100 and z=0 at a very low packing fraction η=0.01. The obtained results are shown in Figure 11(a) for the system with ε=80, and in Figure 11(b) for the system with ε=8. From the behavior of the red lines, which correspond to $g_{zz}(r)$, at small r, it is evident that there is no clustering in the neutral component.
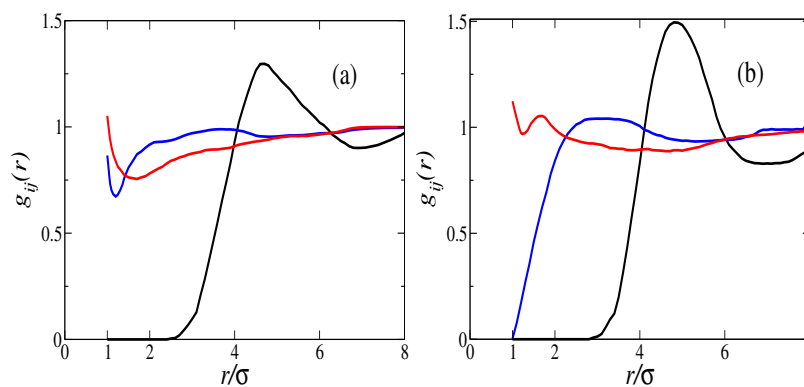

FIG. 11. (Color in online) Partial pair correlations $g_{ij}(r)$ for the binary PM simulations with Z=100, z=0, and η=0.01. Case (a): ε=80, and case (b): ε=8. The functions $g_{ZZ}(r)$ for the charged colloid-charged colloid are shown as black lines, $g_{Zz}(r)$ for the charged colloid-neutral colloid are shown as blue lines, and $g_{zz}(r)$ for the neutral colloid-neutral colloid are shown as red lines.

Appendix D: Colloid-Colloid Pair Interaction Potentials of the Averaged Force

We calculated colloid-colloid interaction potentials explicitly in the PM simulation runs D_1, and D_2, and in the Yukawa-DLVO runs D_1Y, and D_2Y. For this purpose, two colloids of charge $q^{(Z)}=100e$ were placed along the diagonal of the simulation box of size L at a separation distance r. First, the canonically averaged total colloid-colloid interaction force $F_{ZZ}((r)$ was calculated for a set of r varied between 1σ and 4σ. This force includes the direct interaction between the fixed colloids, the electrostatic interaction with other charged colloids and counterions, and the entropic force arising from the collisions with other colloids and counterions. As a remark, a full average has been performed here over all remaining particles. The electrostatic and entropic forces are defined in Appendix A. In the Yukawa-DLVO runs with no counterions, the total colloid-colloid interaction force F_{ZZ}^Y includes only the direct interaction between the colloids, and the electrostatic and entropic interaction with other colloids. Second, the obtained total force is integrated over the separation distance r to get the interaction potential of the averaged force $U_{ZZ}(r)$ in the PM runs, and $U_{ZZ}^Y(r)$ in the Yukawa-DLVO runs. Third, we repeat this procedure for another pair of fixed charges $q^{(Z)}=100e$ and $q^{(z)}=0$, as well as for $q^{(z)}=0$ and $q^{(z)}=0$, to calculate the interactions $U_{Zz}(r)$ and $U_{zz}(r)$ for the PM runs, and $U_{Zz}^Y(r)$ and $U_{zz}^Y(r)$ for the Yukawa-DLVO runs. The resulting colloid-colloid interaction potentials for the averaged force are plotted in Figure 12.
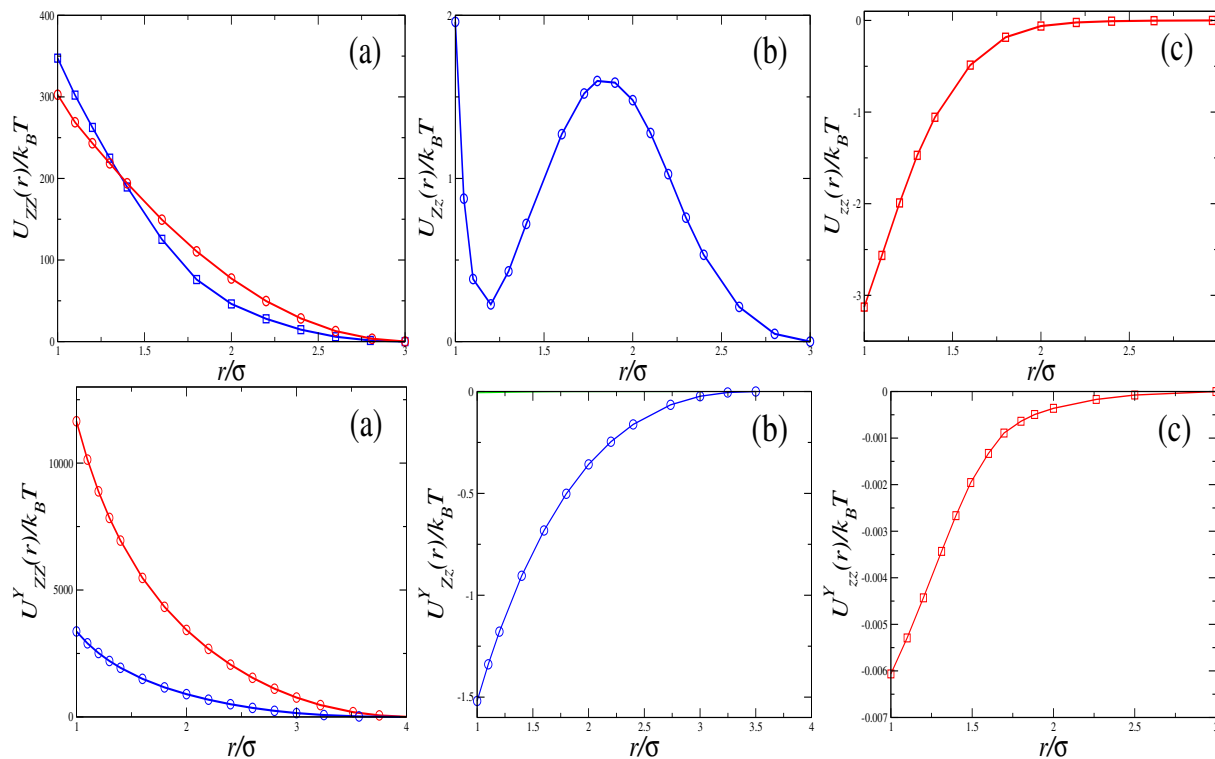
FIG. 12. (Color in online) Upper row- pair interaction potentials $U_{ij}(r)/(k_BT)$ between two fixed colloids in the PM runs. (a) Interaction potentials between the fixed colloids with $q^{(Z)}$=100e in the run D_1 (red line with circles), and in the run D_2 (blue line with squares). (b) The interaction potential $U_{Zz}(r)$ between the fixed colloids with $q^{(Z)}$=100e and $q^{(z)}$=0 in the run D_2. (c) The interaction potential $U_{zz}(r)$ between the fixed colloids with $q^{(z)}$=0 and $q^{(z)}$=0 in the run D_2. Bottom row- the same as in the upper row, but now for the Yukawa-DLVO runs.

REFERENCES

[1] P. N. Pusey, *Colloidal suspensions* in Liquids, Freezing and Glass Transition, Les Houches Session 51, edited by J.-P. Hansen, D. Levesque, and J. Zinn-Justin, (North-Holland, Amsterdam) **2**, 763-931 (1991).

[2] A. Ivlev, H. Löwen, G. Morfill, and C. P. Royall, *Complex plasmas and colloidal dispersions: particle-resolved studies of classical liquids and solids*, Series in Soft Condensed Matter **5**, ISBN: 978-981-4350-06-8, (2012), https://doi.org/10.1142/8139.

[3] L. F. Rojas-Ochoa, R. Castaneda-Priego, V. Lobaskin, A. Stradner, F. Scheffold, and P. Schurtenberger, *Density dependent interactions and structure of charged colloidal dis-*

persions in the weak screening regime, Phys. Rev. Lett. **100**, 178304 (1-4) (2008), https://doi.org/10.1103/PhysRevLett.100.178304.

[4] J. M. Mendez-Alcaraz, B. Daguanno, and R. Klein, *The structure of binary-mixtures of charged colloidal suspensions*, Physica A - Statistical Mechanics and its applications **178**, 421-443 (1991), https://doi.org/10.1016/0378-4371(91)90031-7.

[5] B. D'Aguanno, R. Krause, J. M. Mendez-Alcaraz, and R. Klein, *Structure factors of charged bidispersed colloidal suspensions*, J. Phys. Condens. Matter **4**, 3077-3086 (1992), https://doi.org/10.1088/0953-8984/4/12/007.

[6] P. Wette, H. J. Schoepe, and T. Palberg, *Enhanced crystal stability in a binary mixture of charged colloidal spheres*, Phys. Rev. E **80**, 021407 (1-12) (2009), https://doi.org/10.1103/PhysRevE.80.021407.

[7] S. D. Finlayson and P. Bartlett, *Non-additivity of pair interactions in charged colloids*, J. Chem. Phys. **145**, 034905 (1-10) (2016), https://doi.org/10.1063/1.4959122.

[8] L. Javidpour, B. A. Losdorfer, R. Podgornik, and A. Naji, *Role of metallic core for the stability of virus-like particles in strongly coupled electrostatics*, Scientific Reports **9**, 3884 (1-13) (2019), https://doi.org/10.1038/S41598-019-39930-8.

[9] F. Smallenburg, N. Boon, M. Kater, M. Dijkstra, and R. van Roij, *Phase diagrams of colloidal spheres with a constant zeta-potential*, J. Chem. Phys. **134**, 074505 (1-8) (2011), https://doi.org/10.1063/1.3555627.

[10] J. Dzubiella, J. Chakrabarti, and H. Löwen, *Tuning colloidal interactions in subcritical solvents by solvophobicity: Explicit versus implicit modeling*, J. Chem. Phys. **131**, 044513 (1-5) (2009), https://doi.org/10.1063/1.3193557.

[11] M. Dijkstra, R. van Roij, and R. Evans, *Phase diagram of highly asymmetric binary hard-sphere mixtures*, Phys. Rev. E **59**, 5744-5771 (1999), https://doi.org/10.1103/physreve.59.5744.

[12] R. Roth, *Fundamental measure theory for hard-sphere mixtures: a review*, J. Phys. Condens. Matter **22**, 063102 (1-18) (2010), https://doi.org/10.1103/PhysRevE.91.052121.

[13] N. Heptner and J. Dzubiella, *Equilibrium structure and fluctuations of suspensions of colloidal dumbbells*, Molecular Physics **113**, 2523-2530 (2015), http://dx.doi.org/10.1080/00268976.2015.102260.

[14] S. A. Barr and E. Luijten, *Effective interactions in mixtures of silica microspheres and polystyrene nanoparticles*, Langmuir **22**, 7152-7155 (2006), https://doi.org/10.1021/la061291d.

[15] A. T. Chan and J. A. Lewis, *Electrostatically tuned interactions in silica microsphere- polystyrene nanoparticle mixtures*, Langmuir **21**, 8576-8579 (2005), https://doi.org/10.1021/la0510073.

[16] V. Tohver, J. E. Smay, A. Braem, P. V. Braun, and J. A. Lewis, *Nanoparticle halos: A new colloid stabilization mechanism*, Proc. Natl. Acad. Sci. USA **98**, 8950-8954 (2001), https://doi.org/10.1073/pnas.151063098.

[17] V. Tohver, A. Chan, O. Sakurada, and J. A. Lewis, *Nanoparticle engineering of complex fluid behavior*, Langmuir **17**, 8414-8421 (2001), https://doi.org/10.1021/la011252w.

[18] J. Liu and E. Luijten, *Rejection-free geometric cluster algorithm for complex fluids*, Phys. Rev. Lett. **92**, 035504 (1-4) (2004), https://doi.org/10.1103/PhysRevLett.92.035504.

[19] J. Liu and E. Luijten, *Generalized geometric cluster algorithm for fluid simulation*, Phys. Rev. E **71**, 066701 (1-12) (2005), https://doi.org/10.1103/PhysRevE.71.066701.

[20] J. Liu and E. Luijten, *Stabilization of colloidal suspensions by means of highly charged nanoparticles*, Phys. Rev. Lett. **93**, 247802 (1-4) (2004), https://doi.org/10.1103/PhysRevLett.93.247802.

[21] S. Karanikas and A. A. Louis, *Dynamic colloidal stabilization by nanoparticle halos*, Phys. Rev. Lett. **93**, 248303 (1-4) (2004), https://doi.org/10.1103/PhysRevLett.93.248303.

[22] A. A. Louis, E. Allahyarov, H. Löwen, and R. Roth, *Effective forces in colloidal mixtures: from depletion attraction to accumulation repulsion*, Phys. Rev. E **65**, 061407 (1-11) (2002), https://doi.org/10.1103/PhysRevE.65.061407.

[23] E. N. Scheer and K. S. Schweizer, *Haloing, flocculation, and bridging in colloid-nanoparticle suspensions*, J. Chem. Phys. **128**, 164905 (1-15) (2008), https://doi.org/10.1063/1.2907721.

[24] D. Herman and J. Y. Walz, *Stabilization of Weakly Charged Microparticles Using Highly Charged Nanoparticles*, Langmuir **29**, 5982-5994 (2013), https://doi.org/10.1021/la400699g.

[25] H. Huang and E. Ruckenstein, *Repulsive force between two microparticles decorated with highly charged nanoparticles*, Colloids and Surfaces A: Physicochemical and Engineering Aspects **436**, 862-867 (2013), https://doi.org/10.1016/j.colsurfa.2013.08.024.

[26] N. M. Zubir, A. Badarudin, S. N. Kazi, M. Misran, A. Amiri, R. Sadri, and S. Khalid, *Experimental investigation on the use of highly charged nanoparticles to improve the stability of weakly charged colloidal system*, J. Colloid and Interface Science **454**, 245-255 (2015), https://doi.org/10.1016/j.jcis.2015.05.019.

[27]B. M. Weight and A. R. Denton, *Structure and stability of charged colloid-nanoparticle mixtures*, J. Chem. Phys. **148**, 114904 (1-11) (2018), https://doi.org/10.1063/1.5004443.

[28]A. R. Denton, *Effective electrostatic interactions in colloid-nanoparticle mixtures*, Phys. Rev. E **96**, 062610 (1-14) (2017), https://doi.org/10.1103/PhysRevE.96.062610.

[29]H. J. M. Hanley, G. C. Straty, and P. Lindner, *Order in a simple colloidal mixture suspension*, Physica A **174**, 60-73 (1991), https://doi.org/10.1016/0378-4371(91)90417-B.

[30]M. E. Leunissen, C. G. Christova, A. P. Hynninen, C. P. Royall, A. I. Campbell, A. Imhof, M. Dijkstra, R. van Roij, and A. van Blaaderen, *Ionic colloidal crystals of oppositely charged particles*, Nature **437**, 235-240 (2005), https://doi.org/10.1038/nature03946.

[31]G. J. Ojeda-Mendoza, A. Moncho-Jorda, P. Gonzalez-Mozuelos, C. Haro-Perez, and L. F. Rojas-Ochoa, *Evidence of electrostatic-enhanced depletion attraction in the structural properties and phase behavior of binary charged colloidal suspensions*, Soft Matter **14**, 1355-1364 (2018), https://doi.org/10.1039/c7sm02220d.

[32]S. Savarala, S. Ahmed, M. A. Ilies, and S. L. Wunder, *Stabilization of Soft Lipid Colloids: Competing Effects of Nanoparticle Decoration and Supported Lipid Bilayer Formation*, ACS Nano **5**, 2619-2628 (2011), https://doi.org/10.1021/nn1025884.

[33]B. Q. Yang, F. Gao, Z. Y. Li, M. Y. Li, L. Chen, Y. Guan, G. Liu, and L. H. Yang, *Selective Entropy Gain-Driven Adsorption of Nanospheres onto Spherical Bacteria Endows Photodynamic Treatment with Narrow-Spectrum Activity*, J. Phys. Chem. Lett. **11**, 2788-2796 (2020), https://doi.org/10.1021/acs.jpclett.0c00287.

[34]J. M. Mendez-Alcaraz, B. D'Aguano, and R. Klein, *Structure of binary colloidal mixtures of charged and uncharged spherical particles*, Langmuir **8**, 2913-2920 (1992), https://doi.org/10.1021/la00048a012.

[35]C. Caccamo, M. Varisto, M. A. Floriano, E. Caponetti, R. Triolo, and G. Lucido, *Phase stability of dense multicomponent charged and uncharged hard-sphere fluid mixtures*, J. Chem. Phys. **98**, 1579-1587 (1993), https://doi.org/10.1063/1.464274.

[36]R. Garibay-Alonso, J. M. Mendez-Alcaraz, and R. Klein, *Phase separation of binary liquid mixtures of hard spheres and Yukawa particles*, Physica A **235**, 159-169 (1997), https://doi.org/10.1016/S0378-4371(96)00337-8.

[37]H. Löwen, P. A. Madden, and J. P. Hansen, *An ab initio description of counterion screening in colloidal suspensions*, Phys. Rev. Lett. **68**, 1081-1084 (1992), https://doi.org/10.1103/PhysRevLett.68.1081.

[38]M. Fushiki, *Molecular-dynamics simulations for charged colloidal dispersions*, J. Chem. Phys. **97**, 6700-6713 (1992), https://doi.org/10.1063/1.463676.

[39]H. Löwen, J. P. Hansen, and P. A. Madden, *Nonlinear counterion screening in colloidal suspensions*, J. Chem. Phys. **98**, 3275-3289 (1993), https://doi.org/10.1063/1.464099.

[40]H. Löwen and E. Allahyarov, *Role of effective triplet interactions in charged colloidal suspensions*, J. Phys. Condens. Matter **10**, 4147-4160 (1998), https://doi.org/10.1088/0953-8984/10/19/003.

[41]C. Russ, H. H. von Grünberg, M. Dijkstra, and R. van Roij, *Three-body forces between charged colloidal particles*, Phys. Rev. E **66**, 011402 (1-12) (2002), https://doi.org/10.1103/PhysRevE.66.011402.

[42]H. Löwen and G. Kramposthuber, *Optimal effective pair potential for charged colloids*, Europhys. Lett. **23**, 637-678 (1993), https://doi.org/10.1209/0295-5075/23/9/009.

[43]M. C. Barbosa, M. Deserno, and C. Holm, *A stable local density functional approach to ion-ion correlations*, Europhys. Lett. **52**, 80-86 (2000), https://doi.org/10.1209/epl/i2000-00407-y.

[44]M. C. Barbosa, M. Deserno, C. Holm, and R. Messina, *Screening of spherical colloids beyond mean field: A local density functional approach*, Phys. Rev. E **69**, 051401 (1-9) (2004), https://doi.org/10.1103/PhysRevE.69.051401.

[45]J.-P. Hansen and H. Löwen, *Effective interactions between electric double-layers*, Annual Reviews of Physical Chemistry **51**, 209-242 (2000), https://doi.org/10.1146/annurev.physchem.51.1.209.

[46]L. Belloni, *Colloidal interactions*, J. Phys. Conf. Matter **12**, R549-R587 (2000), https://doi.org/10.1088/0953-8984/12/46/201.

[47]P. Linse, *Simulation of charged colloids in solution, Advanced Computer Simulation Approaches Soft Matter Sciences II*, Book Series: Advances in Polymer Science **185**, 111-162 (2005), https://doi.org/10.1007/b136795.

[48]A. Torres, A. Cuetos, M. Dijkstra, R. and van Roij, *Sedimentation of charged colloids: The primitive model and the effective one-component approach*, Phys. Rev. E **75**, 041405 (1-8) (2007), https://doi.org/10.1103/PhysRevE.75.041405.

[49]M. Dijkstra, *Computer simulations of charge and steric stabilized colloidal suspensions*, Current Opinion in Colloid & Interface Science **6**, 372-382 (2001), https://doi.org/10.1016/S1359-0294(01)00106-6.

[50]M. Quesada-Perez, E. Gonzales-Tovar, A. Martin-Molina, M. Lozada-Cassou, and R. Hidalgo-Alvarez, *Overcharging in Colloids: Beyond the Poisson-Boltzmann Approach*, Chem. Phys. Chem. **4**, 234-248 (2003), https://doi.org/10.1002/cphc.200390040.

[51]R. Messina, *Electrostatics in soft matter*, J. Phys. Condens. Matter **21**, 113102 (1-18) (2009), https://doi.org/10.1088/0953-8984/21/11/113102.

[52]E. Allahyarov and H. Löwen, *Influence of solvent granularity on the effective interaction between charged colloidal suspensions*, Phys. Rev. E **63**, 041403 (1-13) (2001), https://doi.org/10.1103/PhysRevE.63.041403.

[53]R. Castaneda-Priego, L. F. Rojas-Ochoa, V. Lobaskin, and J. C. Mixteco-Sanchez, *Macroion correlation effects in electrostatic screening and thermodynamics of highly charged colloids*, Phys. Rev. E **74**, 051408 (1-6) (2006), https://doi.org/10.1103/PhysRevE.74.051408.

[54]E. Allahyarov, H. Löwen, and S. Trigger, *Effective forces between macroions: the cases of asymmetric macroions and added salt*, Phys. Rev. E **57**, 5818-5824 (1998), https://doi.org/10.1103/PhysRevE.57.5818.

[55]M. Dijkstra, J. W. Zwanikken, and R. van Roij, *Sedimentation of binary mixtures of like- and oppositely charged colloids: the primitive model or effective pair potentials?*, J. Phys. Condens. Matter **18**, 825-836 (2006), https://doi.org/10.1088/0953-8984/18/3/005.

[56]E. Allahyarov and H. Löwen, *Nonadditivity in the effective interactions of binary charged colloidal suspensions,* J. Phys. Condens. Matter **21**, 424117 (1-7) (2009), https://doi.org/10.1088/0953-8984/21/42/424117.

[57]E. Allahyarov, H. Löwen, and A. R. Denton, *Structural correlations in highly asymmetric binary charged colloidal mixtures*, Phys. Chem. Chem. Phys. **24**, 15439-15451 (2022), https://doi.org/10.1039/D2CP01343F.

[58]A. F. Demirors, J. C. P. Stiefelhagen, T. Vissers, F. Smallenburg, M. Dijkstra, A. Imhof, and A. van Blaaderen, *Long-ranged oppositely charged interactions for designing new types of colloidal clusters*, Phys. Rev. X **5**, 021012 (1-12) (2015), https://doi.org/10.1103/PhysRevX.5.021012.

[59]Y. Avni, R. Podgornik, and D. Andelman, *Critical behavior of charge-regulated macro-ions*, J. Chem. Phys. **153**, 024901 (1-11) (2020), https://doi.org/10.1063/5.0011623.

[60]E. Allahyarov, I. D'Amico, and H. Löwen, *Attraction between like-charged macroions by Coulomb depletion*, Phys. Rev. Lett. **81**, 1334-1337 (1998), https://doi.org/10.1103/PhysRevLett.81.1334.

[61]E. Allahyarov, G. Gompper, and H. Löwen, *Attraction between DNA molecules mediated by multivalent ions*, Phys. Rev. E **69**, 041904 (1-13) (2004), https://doi.org/10.1103/PhysRevE.69.041904.

[62]J. Lekner, *Summation of dipolar fields in simulated liquid-vapour interfaces*, Physica A **157**, 826-838 (1989), https://doi.org/10.1016/0378-4371(89)90068-X.

[63]J. Lekner, *Summation of Coulomb fields in computer-simulated disordered systems*, Physica A **176**, 485-498 (1991), https://doi.org/10.1016/0378-4371(91)90226-3.

[64]M. Mazars, *Lekner summations*, J. Chem. Phys. **115**, 2955-2965 (2001), https://doi.org/10.1063/1.1386904.

[65]J. Z. Wu, D. Bratko, H. W. Blanch, and J. M. Prausnitz, *Monte Carlo simulation for the potential of mean force between ionic colloids in solutions of asymmetric salts*, J. Chem. Phys. **111**, 7084-7094 (1999), https://doi.org/10.1063/1.480000.

[66]J. Wu, D. Bratko, and J. M. Prausnitz, *Interaction between like-charged colloidal spheres in electrolyte solutions*, Proc. Natl. Acad. Sci. USA **95**, 15169-15172 (1998), https://doi.org/10.1073/pnas.95.26.1516.

[67]Y.-R. Chen and C.-L. Lee, *A cell-model study on counterion fluctuations in macroionic systems: effect of non-extensiveness in entropy*, Phys. Chem. Chem. Phys. **16**, 297-303 (2014), https://doi.org/10.1039/C3CP53318B.

[68]A. Gonzalez-Calderon, E. Gonzalez-Tovar, and M. Lozada-Cassou, *Very long-range attractive and repulsive forces in model colloidal dispersions*, Euro. Phys. **227**, 2375-2390 (2019), https://doi.org/10.1140/epjst/e2018-800089-0.

[69]Y. Mao, M. E. Cates, H. N. W. Lekkerkerker, *Depletion force in colloidal systems*, Physica A **222**, 10-24 (1995).

$S_{ii}(k)$

k

(a)

(c)

(a)

(c)

(b)